

Net Pay Application for Nuclear Magnetic Resonance, Nugget Sandstone,
Wyoming Thrust Belt

William J. Sercombe

Amoco Production Co., Houston, Texas

Bryan R. Anderson

Amoco Production Co., Denver, Colorado

Abstract

Nuclear Magnetic Resonance (N.M.R.) test results from the Jurassic Nugget sandstone in the Wyoming thrust belt were combined with other core tests to develop net pay criteria that would reflect water cut and deliverability in addition to hydrocarbon pore volume. The producing characteristics of the Nugget sandstone had previously been correlated to eolian dune facies in the first several years of thrust belt exploration. Inconsistencies in facies-to-pay correlations from new discoveries and longer production histories required a new method to evaluate net pay that would evaluate the impact of connate water saturation on reservoir behavior.

This N.M.R. pay method approach integrates relative permeability, capillary pressure and N.M.R. test evaluations and resultant estimates of reservoir behavior affected by connate water saturation. These tests quantify fractional flow, pore throat size, and relative permeability for any selected water saturation value. The N.M.R. test results partition total porosity by calculating what percentage of the pore space will flow water as determined by the other core tests for selected values of water saturation. Since N.M.R. relates porosity to other core tests, wireline log porosity values can be correlated to reservoir behavior.

Regression analysis on a suite of samples will calculate a linear equation for the percentage of porosity that partitions predicted reservoir behavior as a function of total porosity. The intercept accounts for the difference in connate water binding behavior in a range of porosities for a given rock type.

Final net pay is calculated on a log strip chart that overlays total porosity, the partitioned pore space and water saturation curves. The deliverability and water cut characteristics (reservoir behavior) are predicted when the connate water saturation values fall within the partitioned porosity boundaries. Net pay is selected by eliminating zones with predicted poor reservoir behavior. This net pay method successfully established the relationship between porosity, water saturation and deliverability.

INTRODUCTION

A study was undertaken in three fields in the thrust belt of southwest Wyoming and eastern Utah to explain poor production from low porosity (< 8%) eolian Nugget reservoirs and to determine net pay criteria. The Anschutz Ranch East-East Lobe field, the North Pineview field and the Bessie Bottom field were the fields investigated (Fig. 1). The fields produce retrograde condensate with gas (Fig. 2).

Net pay criteria were difficult to quantify as the best producing well in the study had an average porosity of 6 percent and flowed up to 11 MMCFD from completed intervals. The Bessie Bottom well was a problem producer flowing 2.5 MMCFD with an average porosity of 8 percent (Fig. 3). Cores were available in all three fields. Deliverability differences were initially attributed to eolian dune facies, directional permeability and the presence of gouge-filled fractures compartmentalizing the reservoir (Lindquist, 1983).

DELIVERABILITY STUDY

Extensive cross plotting of k_{max} , k_{90} and $k_{vert.}$ core permeabilities against eolian dune facies, gouge filled fracture intensity and deliverabilities were completed. No correlation could be established between core permeabilities, lithology and deliverability. Core permeabilities were measured at standard conditions to air and are considered 'absolute' permeabilities.

The core from the best producing Anschutz well contained extensive gouge fracturing while the poorly performing Bessie Bottom well had only one gouge-filled fracture per foot. The core also indicated that the Bessie Bottom well had no natural open fractures whereas the Anschutz wells had vertical open fractures.

Permeabilities calculated from pressure transient analysis indicated the Anschutz wells had effective permeabilities of 8 md./ft, an order of magnitude above the geometric average k_{90} core permeabilities of 0.43 md.. The Bessie Bottom effective permeabilities of 0.05 md./ft. were an order of magnitude less than the average core permeabilities of 0.64 md.

The differences in deliverability were determined to be caused by the presence or absence of natural open fractures. The Anschutz Ranch East-East lobe field experienced an effective permeability enhancement owing to the open fractures observed in core. The open fractures cross cut the pre-existing gouge. Cross plot relationships indicated that gouge filling only impacted core permeabilities when porosities exceeded 15%.

The Bessie Bottom core permeabilities were corrected for the effects of net overburden pressure, Klinkenberg gas slippage and relative permeability. The corrected average core permeability value of 0.04 md./ft. closely matched the calculated effective permeabilities of 0.05 m.d./ft.. The Bessie Bottom reservoir was severely impacted by the lack of permeability enhancement from open fractures and in-situ reservoir conditions (Jones, 1980), (Thomas, 1972).

The presence of natural open fracturing intuitively enhances effective permeability. Tighter reservoirs, without permeability enhancements, can have substantially reduced effective permeability below core permeabilities measured at standard conditions.

Deliverability is a function of connate water saturation in both fractured and unfractured reservoirs. The fractures controlled the magnitude of deliverability for water and hydrocarbons (Sercombe, 1989).

NET PAY STUDY

The complex insitu reservoir behavior in these tight reservoirs and the inconsistencies in deliverability to log and core derived porosity and permeability required a new net pay method. Previous net pay cutoffs were often qualitative and inadequate for predicting reservoir behavior merely by selecting a single porosity and water saturation cutoff.

A net pay method that would relate wireline log porosity and water saturations to insitu reservoir conditions was needed.

Core analyses for relative permeability, permeability loss from net overburden pressure, capillary pressure and nuclear magnetic resonance had been previously compiled for specific uses.

The available core analysis results could provide better answers to in-situ reservoir behavior than standalone wireline log calculations.

The common parameter between core and log measurements was water saturation in capillary pressure and relative permeability tests and the measurement of porosity quality from nuclear magnetic resonance.

RELATIVE PERMEABILITY

The impact of connate water saturation on a two phase gas and water reservoir was calculated from drainage curve results. The drainage testing duplicates the effect of a water filled reservoir having water displaced by hydrocarbon migration. The results plot water saturation from the initial 100% to an irreducible water saturation against the relative permeability of the hydrocarbon. The relative permeability of the hydrocarbon will decrease from 100 percent of total absolute permeability at the value of irreducible water saturation to no permeability at 100 percent water saturation.

The relative permeability curves can be recalculated to a fractional flow curve that plots the water cut or fractional flow of water as a percentage of total fluid flow against water saturation (Fig. 4).

CAPILLARY PRESSURE

Pore throat size, capillary pressure and height above the free water line can be calculated from mercury injection testing. A sample is injected with mercury to duplicate the entry of a non-wetting phase such as a hydrocarbon. The pressure is measured incrementally for increasing percentages of mercury and therefore decreasing percentages of water saturation. The results are a measure of rock quality (Wardlaw, 1976).

NUCLEAR MAGNETIC RESONANCE

N.M.R. testing measures porosity and pore size quality. Hydrogen protons emit an electronic signal that is measured by the Nuclear Magnetic Resonance testing. The strength of the signal is measured as amplitude. Samples in water are subjected to a magnetic field, thereby orienting the hydrogen protons. A second magnetic field is applied to the samples. When the second field is removed, the time for the amplitude of the signal emitted by the hydrogen protons to relax to the previous oriented state is measured in fractions of a second. The strength of the signal is proportional to the number of hydrogen nuclei (protons).

Relaxation time is controlled by by the internal surface area of the pore. Two samples with the same porosity will respond differently depending on the size of the pores as smaller pores will have larger surface area. In effect, the smaller the pores, the faster the decay rate and the shorter the relaxation time.

The rate of decrease of the amplitude, which is the slope of the relaxation curve at any one time, can be expressed in units of 'number of protons per second' which are relaxing. The inverse of this rate (1/rate) is called the relaxation time (T1) and is not simple clock time. Amplitude is a function of total porosity.

Two types of plots can be presented from the data. The first is an amplitude vs. relaxation time plot and the second is the total porosity vs. relaxation time. The amplitude plot on the y axis is amplitude per relaxation time divided by total initial amplitude. N.M.R. is a measure of pore size and not pore throat size. The percentage of microporosity, which binds fluid is the 'bound fluid porosity, (BF)' and likewise the percentage of macroporosity, which will flow fluid is termed the 'free fluid porosity, (FF)'.

N.M.R. PAY METHOD

The initial step in the N.M.R. pay method is to choose a value of water saturation that reflects desired values of relative permeability, fractional flow of water, water cut or pore throat size. The study first chose a value of first significant water production based on fractional flow data. This percentage of water saturation is the value at which the volume of free fluid (water) in the pore spaces is more than can be bound by wetting and pore throats and is thus free to flow. Free flow of water implies decreased permeability to hydrocarbons and this decrease is a continuum with increasing water saturation (Fig. 5). The chosen water saturation value is entered as the percentage of amplitude on the amplitude

(A_i/A_0) plot and the corresponding relaxation time (T_1) is chosen. This value for the relaxation time is entered on the porosity vs (T_1) plot and the porosity value for free fluid porosity is obtained. The free fluid porosity value indicates the percentage of the pore volume which will flow the wetting phase (water) (Fig. 6).

For example, two rock samples may each have 10% porosity but their free fluid porosity will depend on the distribution of pore sizes. The well-sorted sample with uniform large pore throat size may only have 30% of its total porosity that will bind water. The more poorly sorted sample with a range of very small to large pore throat sizes may have 60% of its total porosity bind water. The bound fluid porosities will be 30 and 60 percent respectively. The N.M.R. measurements are reliable only in intergranular porosity types because the technique responds to pore size and not pore throat size. Therefore the technique only is reliable when pore size and pore throat size are directly related.

A suite of rock types for a reservoir are chosen and tested and a range of total porosities and their free fluid porosity values are obtained. The data set is then used to calculate a best fit and a linear equation is derived for free fluid porosity as a function of total porosity.

The terms 'free fluid porosity' and 'bound fluid porosity' reflect the original concept of dividing porosity based on fluid-binding quality. A number of significant water saturation values can be chosen. 'Free' and 'bound' are holdover terms and are not literal. They reflect the relative ends of the water saturation and pore size spectrum. In this study, for

example, the water saturation for 80% fractional flow of water (70% Sw) was chosen as well as the value for first water cut (40% Sw) in order to derive bound fluid porosities BF(70) and BF(40).

BEST FIT ANALYSIS

A linear equation for free fluid porosity as a function of total porosity was calculated from the sample population for both the 40 and 70 percent Sw values. The intercept accounts for the tighter rock binding more water than a porous rock.

The resultant value from using the best fit equation as an algorithm reflects the interaction of both water saturation and porosity as both parameters were used. The water saturation was input in the initial Sw value selection and the porosity was derived from N.M.R.. This is similar to a Buckles relationship and reflects the interaction of connate water saturation and porosity which are critical to understanding deliverability differences (Buckles, 1965).

The porosity and water saturation as a percentage of the total porosity (Porosity * Sw or Buckles number) are calculated and can be plotted on a log strip chart. The derived 'free fluid' value partitions the porosity.

When the Buckles value equals the 'free fluid' value the rock will have the water cut and relative permeability characteristics chosen from the core analysis.

The final linear equations were as follows for the Nugget:

$$\text{Free fluid @ 40\% Sw} = .67 * \text{porosity} - 1.1$$

The first appearance of water cut occurs at 40% Sw.

Free fluid @ 40% Sw = .67 * porosity - 1.1; @ 10% porosity = 5.6% of total porosity.

Bound fluid @ 40% Sw = porosity - (.67 * porosity - 1.1); @ 10 % porosity = 4.4 % of total porosity ie., when the Buckles number or porosity * Sw value exceeds 4.4 % out of a total of the 10 % porosity, the first water cut will appear.

$$\text{Free fluid @ 70\% Sw} = .41 * \text{porosity} - 1$$

The 80 % fractional flow value was found at 70 % Sw.

Free fluid @ 70% Sw = .41 * porosity - 1; @ 10% porosity = 3.1 % of total porosity.

or

Bound fluid @ 70% Sw = porosity - (.41 * porosity - 1); @ 10 % porosity = 6.9 % of total porosity ie., when the Buckles number or porosity * Sw value exceeds 6.9 % out of a total of the 10 % porosity, 80 % fractional flow will occur.

The last step partitions the pore space of the porosity log so that zones of favourable and unfavourable water cut and deliverability could be presented on the log strip chart.

The porosity curve is plotted. The water saturation as a percentage of porosity (porosity * Sw) is plotted as an overlay curve so that hydro-

carbon pore volume is presented. The curves for the bound fluid values were generated and overlain on the first set of curves.

Example:

For a zone with an irreducible water saturation value at the top and a free water line at its base the resultant value would tabulate as follows assuming a constant 10% porosity.

Free fluid @ 70% Sw = .41 * porosity - 1 = 3.1, BF= 10% - 3.1 = 6.9

Free fluid @ 40% Sw = .67 * porosity - 1.1 = 5.6, BF = 10% - 5.6 = 4.4

Zone	Porosity	Sw	Porosity * Sw	BF 40%	BF 70%	
A	10	.2	2	< 4.4	6.9	no water, max. deliverability
B	10	.3	3	< 4.4	6.9	no water, max. deliverability
C	10	.4	4	< 4.4	6.9	no water, max. deliverability
D	10	.44	4.4	= 4.4	< 6.9	first water cut
E	10	.5	5	> 4.4	< 6.9	increasing water cut
F	10	.6	6	> 4.4	< 6.9	increasing water cut
G	10	.69	6.9		= 6.9	80 % fractional flow
H	10	.7	7		> 6.9	almost full water cut
I	10	.8	8		> 6.9	minimal to no deliverability
J	10	.9	9		> 6.9	
K	10	1.0	10		< 6.9	

Zones A, B and C could be completed water free. Zones D thru G would experience increasing water cut and decreasing deliverability. Zones H thru K would be unsuitable for completion due to high water cuts.

Digital curve presentation and calculation will permit the calculation of the porosity, porosity * Sw and bound fluid porosity curves for overlay plots. The zones of desired water cut, relative permeability or other criteria will be shown where the porosity * Sw curve crosses the different BF curves until it matches the porosity curve at 100% water saturation (Fig. 7).

The Bessie Bottom well plot (Fig. 8) could have predicted both the water free completions and better deliverability zones and the zone of 100 % water cut.

CONCLUSIONS

The N.M.R. pay method partitioned zones of deliverability differences in wells. The deliverabilities declined down the gas columns as connate water saturations increased. The strip chart display of the data calculated by the N.M.R. method allowed a visual discrimination of pay and relative gas and water deliverability.

The N.M.R. method calculated and revealed the constantly changing interactions of porosity and water saturation in the gas columns.

REFERENCES

Buckles, R.S., 1965, Correlating and averaging connate water saturation Data: Canadian Institute of Mining, Petroleum and Natural Gas Div., May.

Hayes, K.H. 1976, A discussion of the geology of the southeastern Canadian cordillera and its comparison to the Idaho-Wyoming-Utah fold and thrust Belt, in J.G. Hill, ed., Symposium on Geology of the Cordilleran Hingeline: Rocky Mountain Association of Geologists p.59-82.

Jones, F.O., Owens, W.W., 1980, A laboratory study of low permeability gas sands: Journal of Petroleum Technology, Sept., .1631-1640.

Lindquist, S.J., 1983, Nugget formation reservoir characteristics affecting production in the overthrust belt of southwestern Wyoming: Journal of Petroleum Technology, v. 35, p. 1355-1365.

Sercombe, W.J. 1989, Performance of lower-porosity nugget reservoirs, Anschutz Ranch East, Bessie Bottom, and North Pineview fields, Utah and Wyoming: in Sandstone Reservoirs-1989, Rocky Mountain Association of Geologists p.109-116

Thomas, R.D., Ward, D.C., 1972, Effect of overburden pressure and water saturatoin on gas permeability of tight sandstone Cores: Journal Petroleum Technology, Feb. p. 121-124.

Wardlaw, N.C., Taylor, R.P., 1976, Mercury capillary pressure curves and the interpretation of pore structure and capillary behavior in reservoir rock: Bulletin of Canadian Petroleum Geology, v. 24, June, p.225-262.

A:WJS001.K75

STRATIGRAPHIC COLUMN

WYOMING-IDAHO-UTAH FOLD AND THRUST BELT

AGE	FORMATION OF GROUP	LITHOLOGY	THICKNESS	FACIES		
TERTIARY	SALT LAKE GRP. GREEN RIVER GRP.		0 - 8000'	LAKE BEDS		
	WASATCH GRP.			CONTINENTAL		
CRETACEOUS	UPPER		6000 - 16,000'	CONTIN- ENTAL DELTAIC MARINE		
				ADAVILLE FM.	DELTAIC MARINE	
				HILLIARD FM. ? FRONTIER FM.		
	LOWER		1000 - 10,000'	DELTAIC MARINE		
				ASPEN FM.	DELTAIC MARINE DEL- TAIC	
				BEAR RIVER GRP.		
				GANNETT GRP. ? STUMP ?		
	JURASSIC	PREUSS		500 - 1000'	MARINE LOCALLY RESTRICTED	
JR	TWIN CREEK FM.		1500 - 3500'	MARINE		
TRIASSIC	UPPER		0 - 2000'	CONTINENTAL		
	MIDDLE	ANKAREM	2000 - 7000'	CONTINENTAL		
		THAYNES		MARINE		
	LOWER	WOODSIDE DINWOODY			MARINE	
PERMIAN	PHOSPHORIA		400 - 5000'	MARINE		
PENNSYLVANIAN	WEBER-WEELS TENSLEEP AMSDEN		750 - 4000'	MARINE		
MISSISSIPPIAN	BRAZER	MADISON	1000 - 7000'	MARINE LOCALLY RESTRICTED		
	LODGEPOLE			MARINE		
DEVONIAN	THREE FORKS JEFFERSON	DARBY	500 - 3000'	MARINE		
SILURIAN	LAKETOWN		0 - 2000'	MARINE		
ORDOVICIAN	FISH HAVEN SWAN PEAK	BIGHORN	250 - 2000'	MARINE		
CAMBRIAN	GRADEN CITY ST. CHARLES WORM CREEK NOONAN	GALLATIN	1500 - 5000'	MARINE		
	BLOOMINGTON BLACK SMITH					
	LIFE LANGSTON	GROSVENTRE				
	BRIGHAM	FLATHEAD				
	PRE-CAMBRIAN	SEDIMENT & METASEDIMENT				
	PRE-CAMBRIAN	CRYSTALLINE BASEMENT				

* RESERVOIR STUDIED

Figure 1 - Index Map showing location of studied (black) and nearby Triassic-Jurassic Nugget sandstone fields. Bessie Bottom, Anschutz Ranch East, and North Pineview are hanging wall anticlines in the southern part of the Absaroka thrust sheet. (6 mi. = 9.7 km.)

U.S. GEOLOGICAL SURVEY

UTAH-WYOMING THRUST BELT

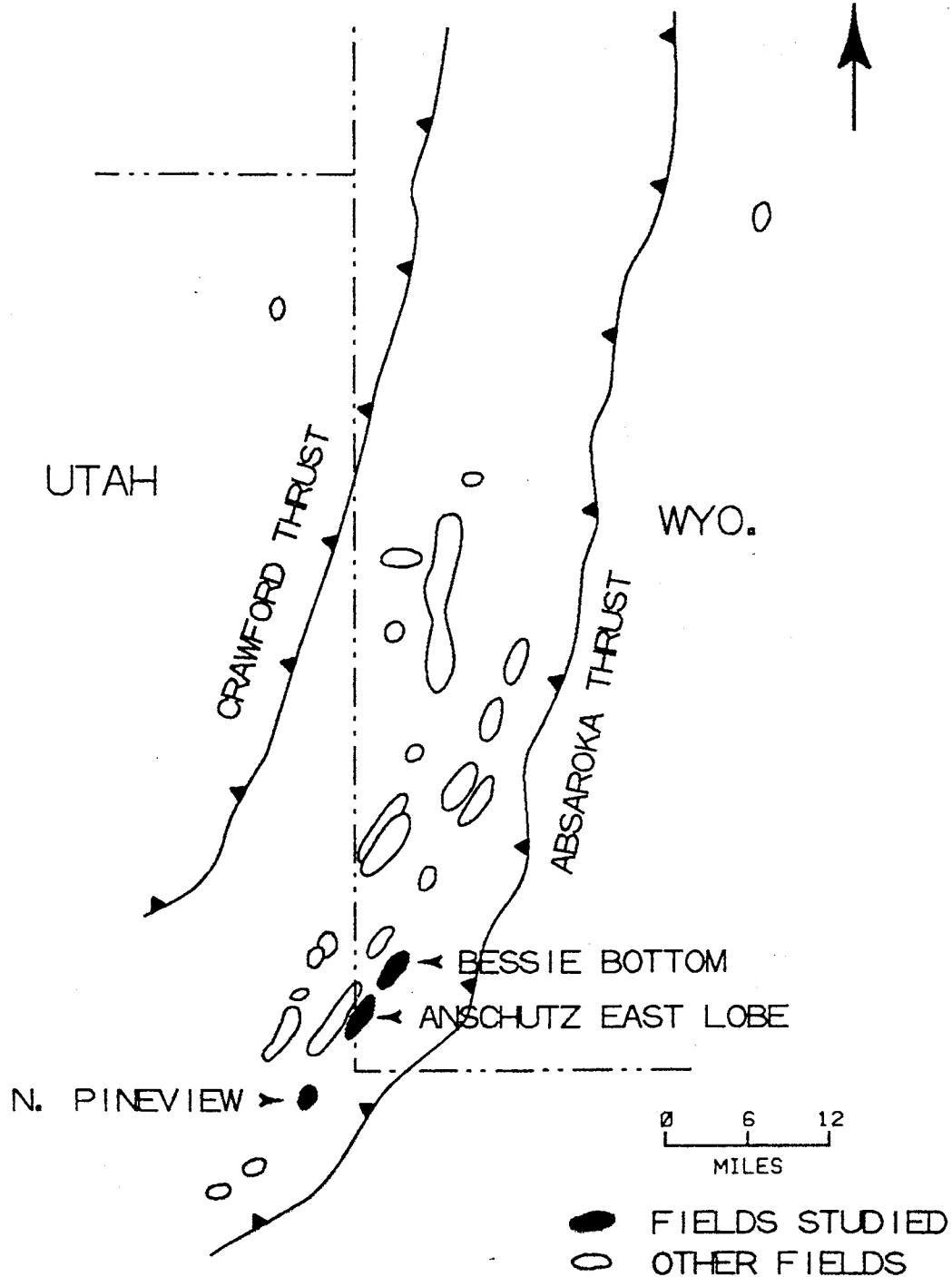


Figure 2 - Stratigraphic column for the Wyoming-Idaho-Utah fold and thrust belt. The Triassic-Jurassic Nugget Formation is an eolian sandstone and one of the principal reservoirs in the Wyoming thrust belt.

GAS COLUMN HEIGHTS ABOVE FREE WATER LINE

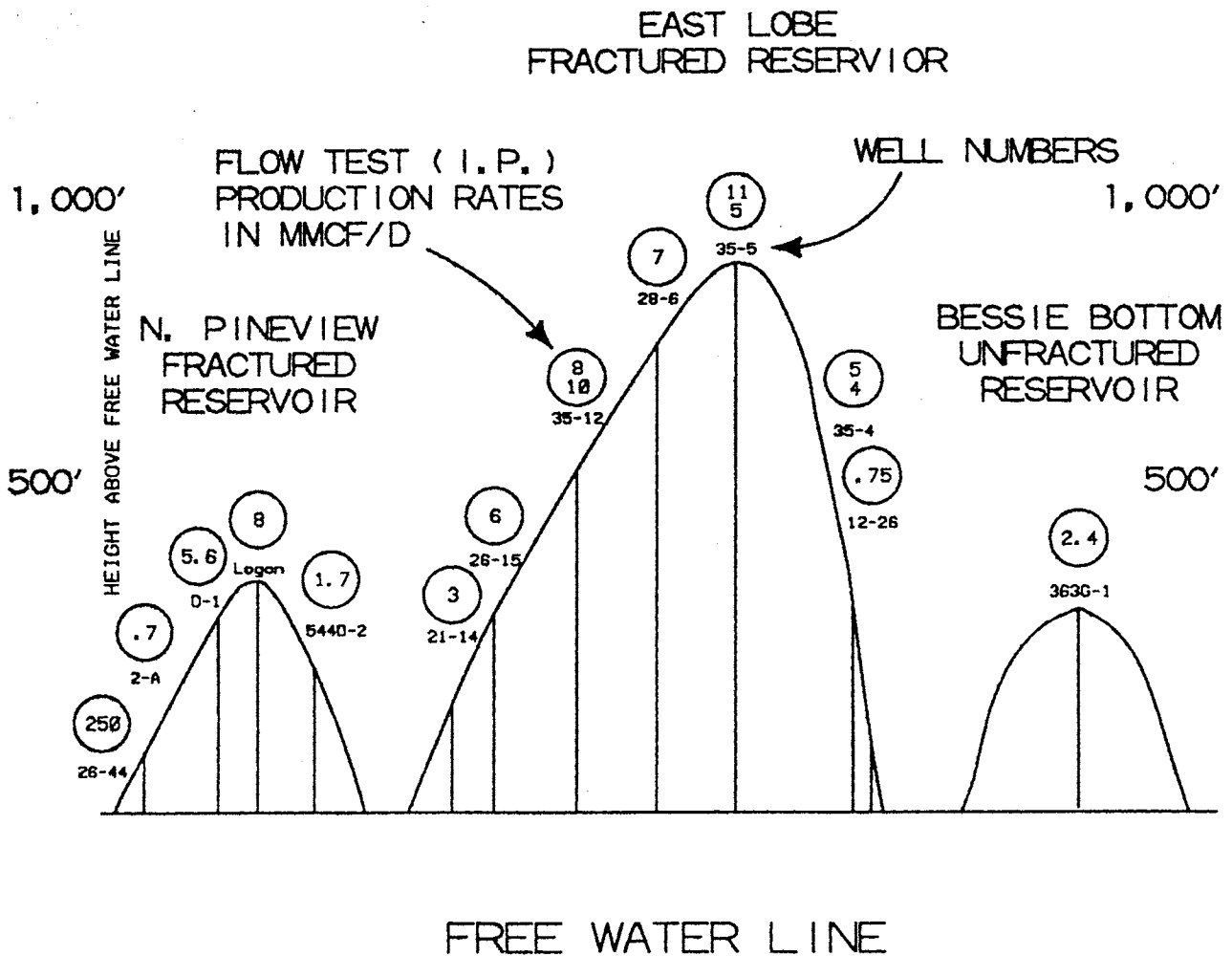
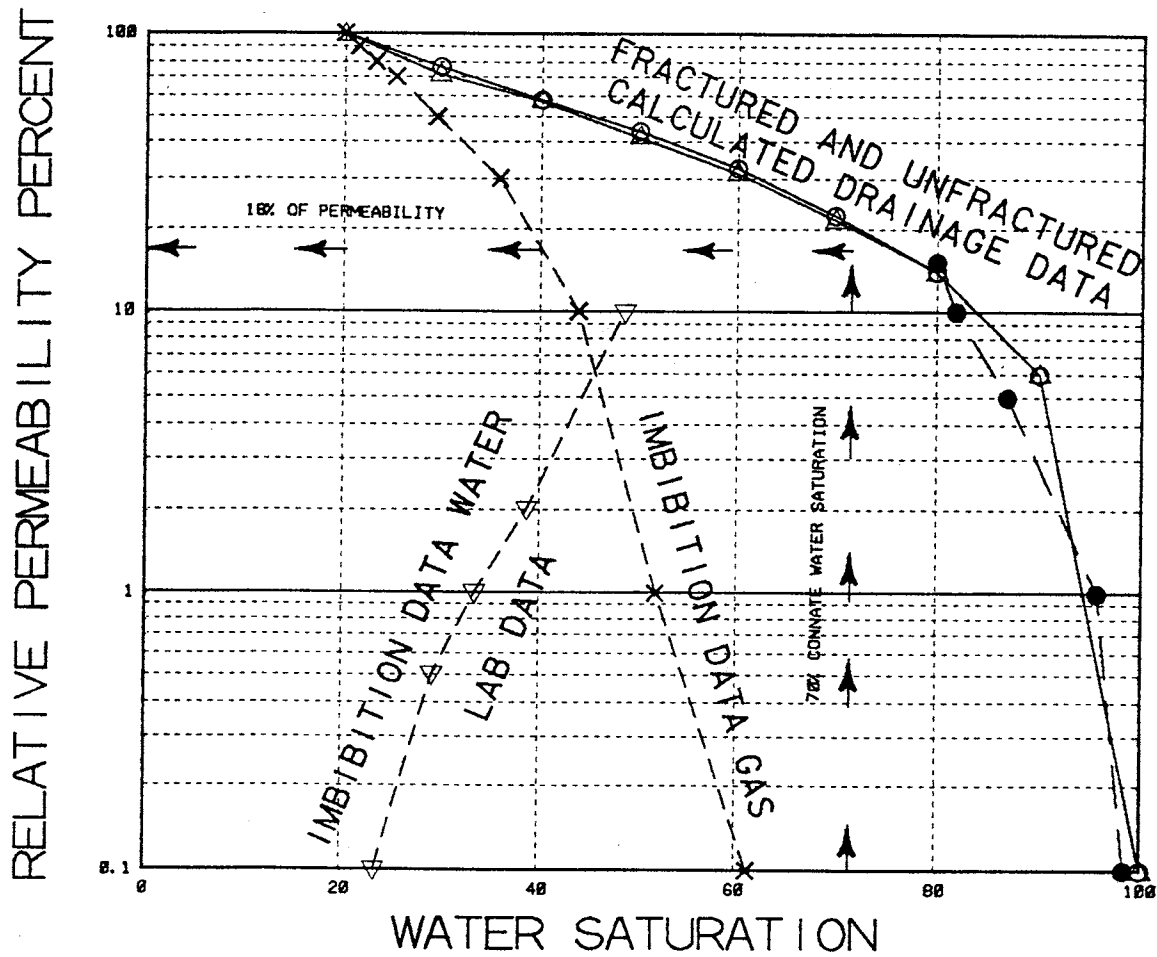


Figure 3 - Heights of gas columns in Nugget sandstone reservoirs, Bessie Bottom, Anschutz Ranch East and North Pineview fields, Wyoming. The deliverability of gas increases with height above free water. Deliverability also is impacted by the relative permeability effects associated with increasing connate water saturations.

WATER-GAS RELATIVE PERMEABILITY

DATA SWIR = 20%



LEGEND

- GAS-OIL
- WELL TEST
- △ WELL TEST BESSIE
- × GAS
- ▽ WATER

Figure 4 - Theoretical relative permeability curve, Nugget sandstone, Bessie Bottom, Anschutz Ranch East and North Pineview fields, Wyoming. The drainage curve was derived empirically from a best fit curve of deliverability versus connate water saturation and allows for correction of lab permeabilities.

NMR NET PAY METHOD

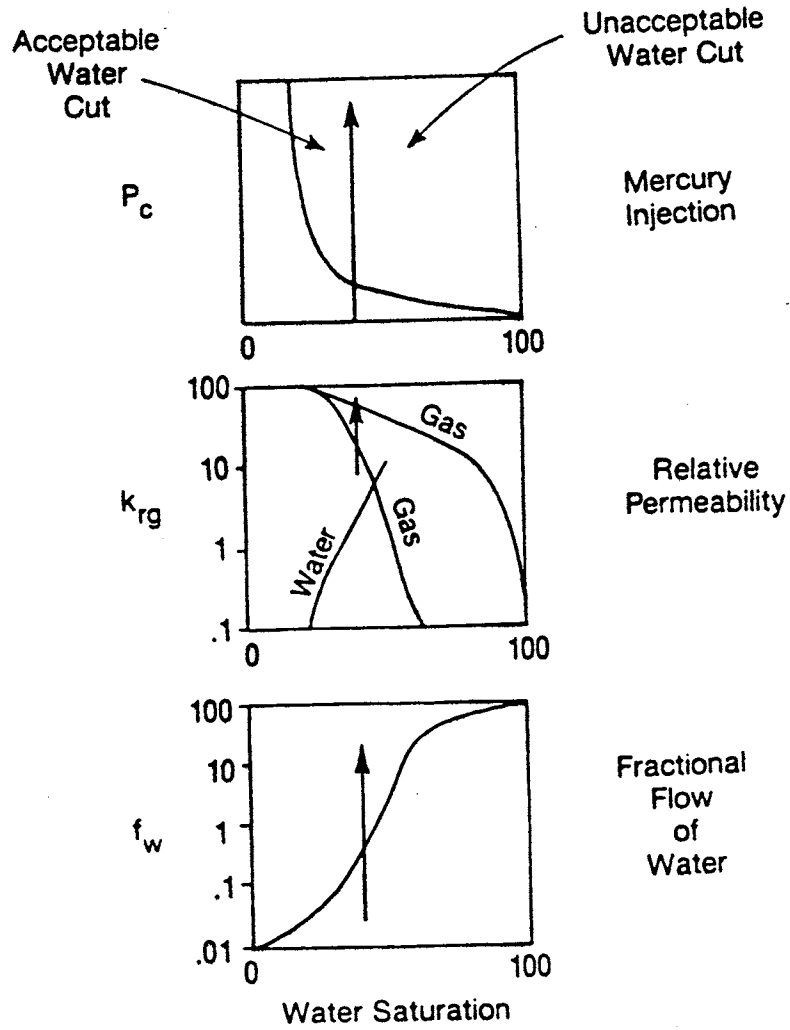


Figure 5 - The first steps in the NMR pay method is to choose values of connate water saturation based on desired effects of fractional flow, water cut, relative permeability or pore throat size.

NMR NET PAY METHOD (cont'd)

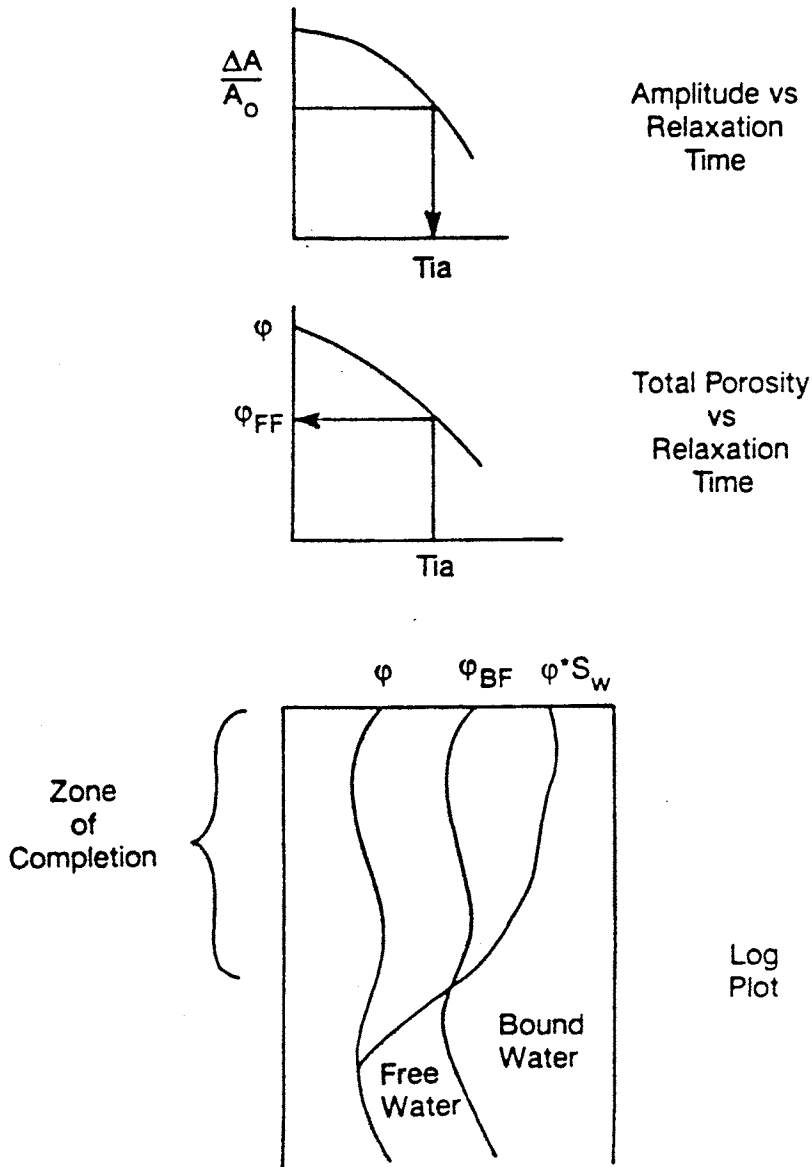


Figure 6 - The final steps in the NMR pay method are to enter the chosen water saturation value as the percentage of amplitude to derive a relaxation time. The relaxation time is entered on the next plot to derive a Bound Fluid Porosity value. Best fit analysis is used to generate a curve to partition pore space.

In this diagram the point where the porosity * S_w curve crosses the bound fluid porosity curve is where the reservoir will behave as chosen for fractional flow and relative permeability.

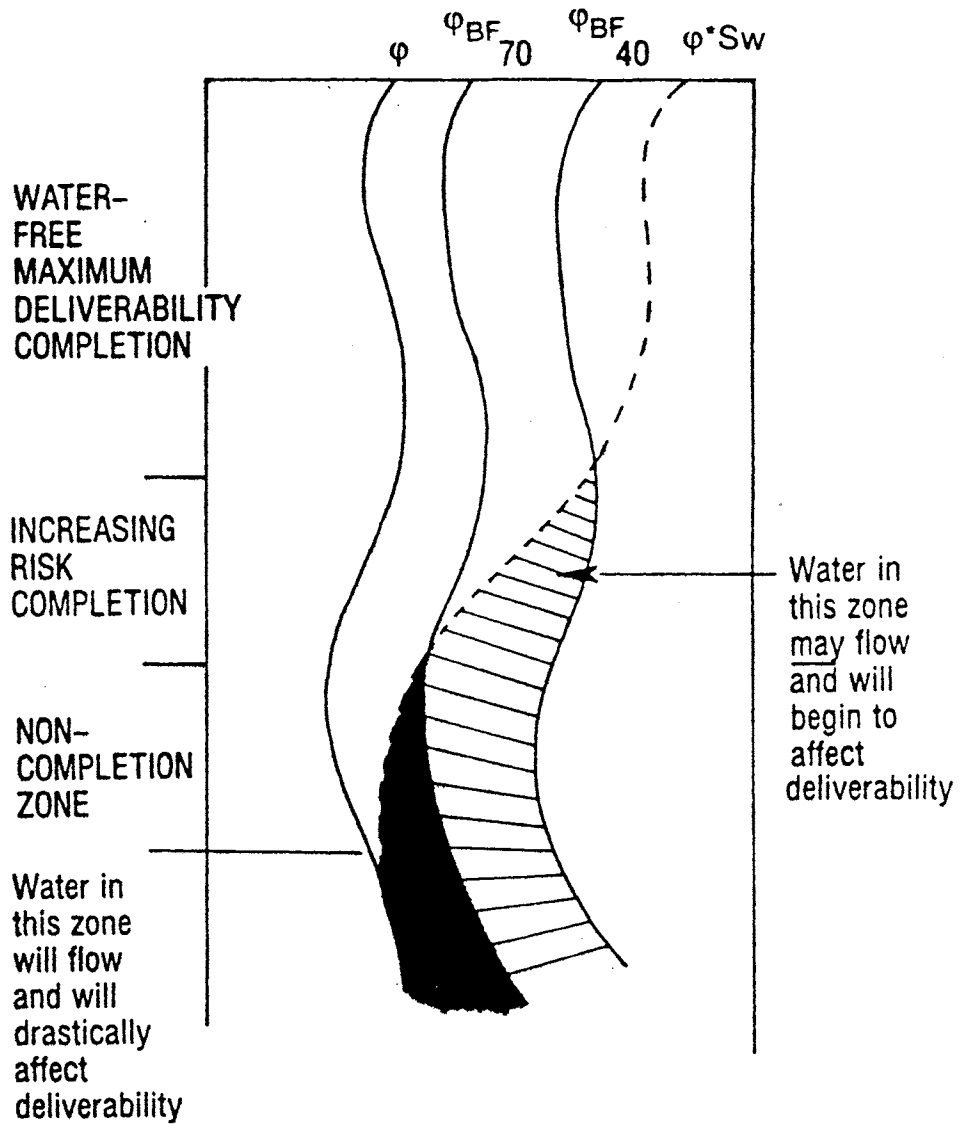


Figure 7 - The curves for reservoir behavior at 70% Sw and 40% Sw are plotted and define zones for completion. The top zone will not flow water and will have maximum deliverability. The zone where Porosity * Sw lies between the BF 40 and BF 70 curves will have lower deliverability and increasing water cut. The lower zone will have minimal deliverability and maximum water cut.

BESSIE BOTTOM WELL

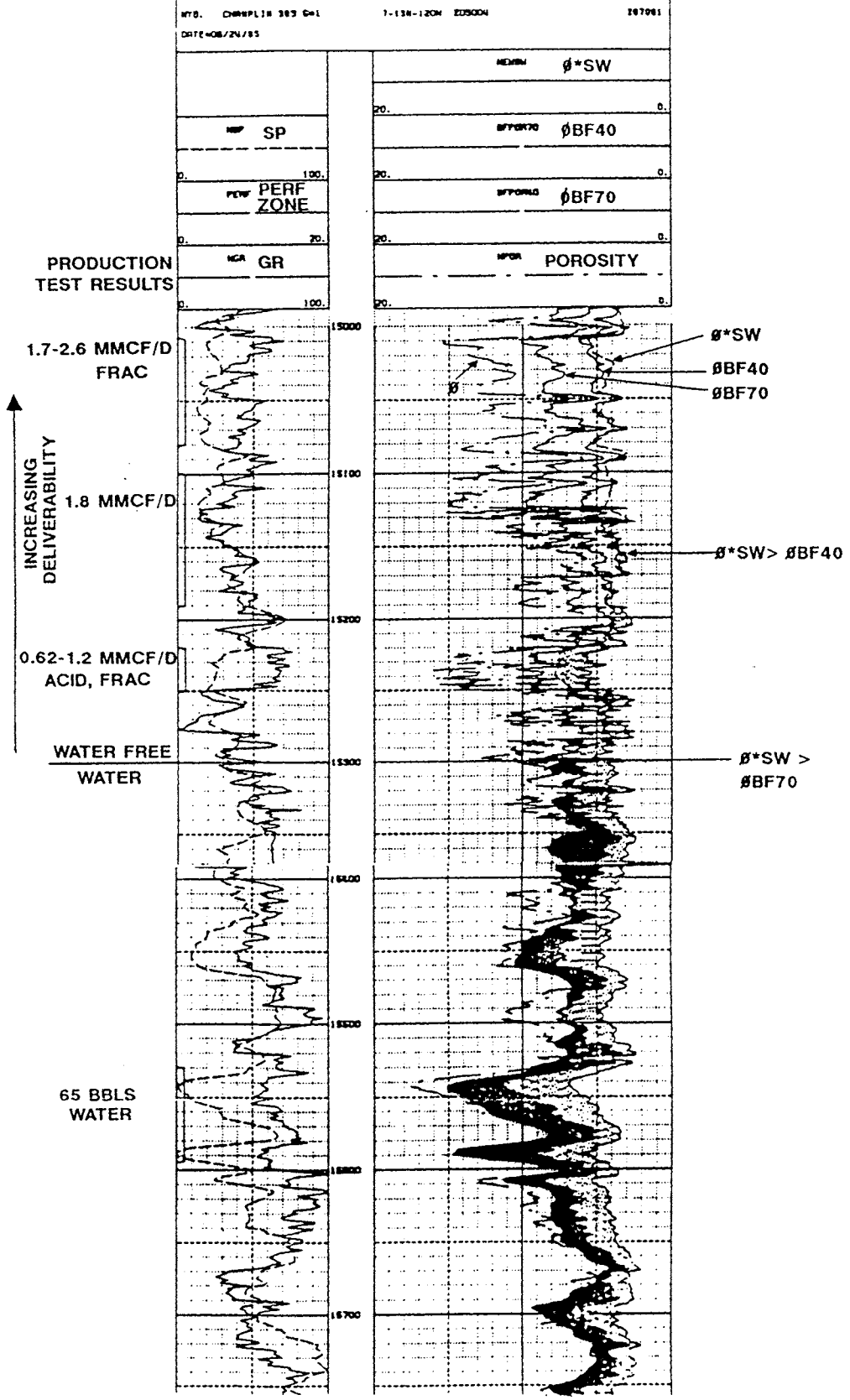


Figure 8 - The Bessie Bottom well deliverabilities could be predicted using the NMR pay method. Maximum deliverability was at the top of the column and water production was obtained at the bottom.

